IEEE Access
Multidisciplinary | Rapid Review | Open Access Journal

Received November 13, 2020, accepted December 5, 2020, date of publication December 11, 2020,
date of current version December 29, 2020.

Digital Object Identifier 10.1109/ACCESS.2020.3044102

An Asynchronous Trajectory Matching Method Based on Piecewise Space-Time Constraints

CHAO LIU[1], JINLEI WANG[2], AICHAO LIU[3], YONGNING CAI[4], AND BO AI[1,5]
[1]College of Geomatics, Shandong University of Science and Technology, Qingdao 266590, China
[2]North China Sea Data and Information Service, Ministry of Natural Resources, Qingdao 266033, China
[3]North China Sea Marine Forecasting Center, Ministry of Natural Resources, Qingdao 266061, China
[4]Jinan Research Institute of Surveying and Mapping, Jinan 250101, China
[5]Key Laboratory of Urban Natural Resources Monitoring and Simulation, Ministry of Natural Resources, Shenzhen 518000, China

Corresponding author: Bo Ai (aibo@sdust.edu.cn)

This work was supported by the National Key Research and Development Program of China under Grant 2017YFC1405002, the National Natural Science Foundation of China under Grant 62071279, the Key Laboratory of Urban Natural Resources Monitoring and Simulation, Ministry of Natural Resources under Grant KF-2019-04-070, and SDUST Research Fund under Grant 2019TDJH103.

ABSTRACT Automatic Identification System (AIS) is an automatic tracking system based on reports provided by AIS transponders, which can report the static and dynamic information of the ship, such as name, call sign, position and speed etc. However, AIS can be manually turned off, making it impossible to find the trajectory of the ship when AIS is turned off, which results in difficulties in maritime supervision. This article uses shore-based radar trajectory data to present a new method of asynchronous trajectory matching based on piecewise space-time constraints (PTSCTM), which is used to reconstruct AIS trajectory and discover the abnormal behavior of ships. The Ramer–Douglas–Peucker (RDP) algorithm is used to extract feature points of the trajectory, and the trajectory is segmented according to feature points. The method uses space-time constraints to determine candidate trajectory matching points in each trajectory segment and calculates the optimal matching point from the candidate set through the space and time distance. The method asynchronously calculates the similarity of trajectory segments from multi-source trajectories and calculates the trajectory similarity to achieve multi-source trajectory matching. The measured data show that the model can effectively measure the similarity of multi-source trajectories to find the optimal radar trajectory as a matching result when AIS is turned off, and the calculation accuracy and efficiency of the model is higher than the existing methods. According to the asynchronous trajectory matching method, the monitoring method of staying ships in the Qingdao lancelet reserve area is proposed. The result shows that many ships stayed in the area through radar signals when AIS was turned off. The result can provide auxiliary support for maritime supervisory and legal departments, which helps to strengthen maritime ship supervision, detect maritime illegal crimes and protect the marine environment.

INDEX TERMS Trajectory similarity, trajectory matching, space-time constraints, ship supervision, the monitoring of nature reserves.

I. INTRODUCTION

The development of shipping makes maritime traffic safety navigation an important research topic and the AIS is the basic means to guarantee the safety of ship navigation. The AIS is an automatic tracking system based on the report of the ship's AIS transponder. It can provide dynamic information such as the ship's position and speed, as well as static information such as ship's type, name and country. Ships with a gross tonnage above 300 gross tonnages in international voyages, ships and passenger ships with cargoes over 500 gross tonnages that are not in international waters must be equipped with AIS [1]. In addition, fishing ships with a length of more than 15 meters and those sailing within the jurisdiction of the European Union (EU) require the AIS [2]. The AIS can represent a global, near a real-time information source, with high accuracy, small constraints and global advantages. The AIS functions include: identifying ships; assisting in tracking targets; simplifying information exchange; providing other auxiliary information to avoid collisions. The use of the AIS helps to strengthen the safety of life at sea, improve the safety and efficiency of

The associate editor coordinating the review of this manuscript and approving it for publication was Gang Mei.

navigation, and protect the marine environment. It has been widely used in marine ship data mining [3], [4], marine ship safety monitoring [5], [6], marine ecological environment supervision [7], and marine search and rescue work [8].

However, given that AIS is a self-reporting system, the crew can close the AIS resulting in the loss of the AIS signal to prevent the surveillance system and its operators from discovering its illegal activities. It has a negative impact on water traffic safety. Since June 1, 2020, the Ministry of Transport has launched a special rectification of the national maritime radio order management to severely crack down on the intentional shutdown of the AIS signal and other acts in China [9]. The use of other sensor signals as a supplement is widely used for the solution of the single instability problem [10]. Shore-based radar can automatically detect the target and return the target's distance, bearing, heading, speed and other information in real time [11]. Radar is an active traditional means of target detection. Although it cannot provide attribute information similar to ship name and country, it has advantages that AIS and other communication methods based on self-reporting methods do not have. Radar can detect targets when the AIS report is turned off. Therefore, it is significant to find dangerous targets and ensure the safety of navigation at sea. Radar is easily affected by the environment, so the accuracy is not high and the target resolution is also difficult. But the active detection method can be used as a supplement to AIS when the signal is turned off. As shown in Fig. 1, when the AIS is manually turned off, the ship may drive to the forbidden area during the course of driving such as prohibited fishing areas, marine nature reserves and reclamation areas, etc. The ship tries to cover their movements through the AIS report, which makes it unable to rely solely on the AIS trajectory to identify its illegal activities. However, the radar as an active detection method can scan and record the trajectory of the ship within the radar detection range when then AIS is turned off.

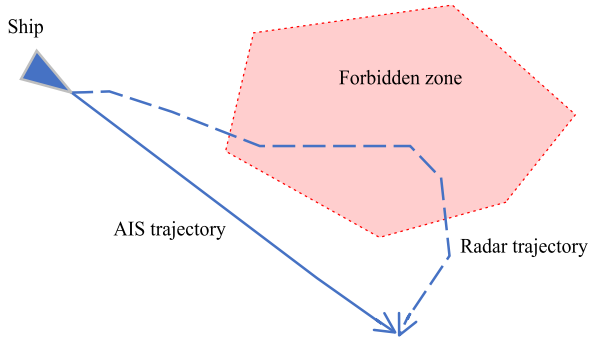

FIGURE 1. When AIS is turned off, the radar trajectory still finds that the ship enters the prohibited area.

Many articles have studied multi-source trajectory matching from the perspective of trajectory association. According to the association principle, it can be divided into two methods, which are statistics-based and fuzzy mathematics. The correlation methods based on statistical methods mainly include NN [12], K-NN [13], MK-NN [14], double threshold [15], the sequential method [16] and so on. Affected by the complexity of the marine environment and the systematic errors, random errors and detection ranges of various measurement methods, the similarity between the local trajectories of different sensors has ambiguity, so ambiguity can be used in related mathematical theories to judge the relevance of trajectories. Chen *et al.* proposed a trajectory association algorithm based on fuzzy similarity, in which the concept of membership was used to describe the similarity of two data and the fuzzy theory was used to calculate the fuzzy comprehensive similarity between possible associated trajectories [17]. Ou *et al.* proposed a multi-factor fuzzy comprehensive decision similarity method to calculate the correlation between two sensors [18]. Guo and Zheng proposed a method for evaluating the similarity of trajectories based on topological information between targets [19]. Mao *et al.* proposed a method to divide the detection target of the sensor into several topological triangle structures combined with the topological four-cross model to define the triangle similarity, thereby measuring the similarity of the trajectory and achieving trajectory association [20]. However, these algorithms are synchronous correlation algorithms and cannot handle such inconsistent sampling data rates. When they are used, the observations are first interpolated to make the data consistent and then trajectory filtering and correlation operations are performed.

The trajectory can be understood as a time series of spatial positions, and there are more and more similarity measurement methods of spatio-temporal trajectories. Typical methods include Frechet distance [21], Hausdorff distance [22], [23], Euclidean distance [24], [25], dynamic time warping (DTW) [26], [27], longest common subsequence (LCS) [28]–[30] and edit distance [31]–[33]. However, these methods emphasize the similarity of spatial position or trajectory shape, while ignoring the time dimension and regard the trajectory as a sequence of points. In terms of spatial-temporal similarity matching, the time-locking method calculates the sum of the distances of two points with the same timestamp but is prone to noise and outliers [34]. Kondor *et al.* proposed that the two points will be regarded as a match only when space and time are close. If two points are close in time, but far apart in space, they are considered impossible to match. Then the unmatched trajectory pairs are directly excluded [35]. Sun *et al.* proposed a trajectory similarity model based on spatial and temporal constraints (STCTS), it set the space-constrained distance and the time-constrained distance for multi-source trajectories, then found matching points, finally calculated the similarity of matching points [36]. The greater the similarity is, the more likely the two trajectories are multi-source trajectories. Gong *et al.* proposed Time Weighted Similarity (TWS) and Space Weighted Similarity (SWS) to calculate the spatial and temporal trajectory similarity of different positioning accuracy, sampling efficiency and length [37]. However, it is sensitive to noise

points and is not suitable for signal loss using the linear interpolation method. It has been developed in recent years based on these similarity measurement methods, which are suitable for the cases where spatio-temporal trajectory matching and where two trajectories are completely sampled and there is no large loss. But it is not applicable when the signal is lost for a long time. Therefore, it is not applicable to the situation where AIS is turned off and the trajectory point is lost.

In identifying AIS erroneous trajectories by radar trajectories, Katsilieris *et al.* proposed a method based on statistical hypothesis testing [38]. This method assumed that the false alarm rate of the radar trajectory is 0, it is considered to be completely correct. The correct trajectory reported by AIS is considered a simple null hypothesis, while the wrong trajectory reported by AIS is a composite alternative hypothesis. By changing the deception jamming distance and the number of radars, the corresponding ROC curve and the expected number of required samples are obtained to make the correct decision. But the ship can simply turn off its AIS signal (perhaps periodically) instead of making an error report to prevent the surveillance system and its operators from discovering illegal activities. At the same time, this method is only suitable for a single target, and cannot handle scenes with multiple targets. At the same time, the interpolation method is used to fill the AIS in the signal loss [39], [40]. The common one is cubic spline interpolation [41] that is suitable for the case where the time interval is short and the trajectory does not change significantly and multiple turns.

This article proposes an asynchronous trajectory matching method based on piecewise space-time constraints for the characteristics of AIS self-reporting and the advantages of radar actively detecting ships. The method uses trajectory similarity based on piecewise space-time constraints (PTSCTS) to calculate the possibility of being the same trajectory. It is intended to realize multi-source trajectory matching between AIS trajectory and radar trajectory when AIS is turned off. Fig. 2 shows the framework of PTSCTM. Data storage uses AIS track data and radar track data. After reading the data, track processing is performed first. Coordinate axis projection is used to make rough judgments and obtain possible matching multi-source trajectories. The methods using RDP trajectory compression algorithm are used to divide the original AIS trajectories into short and non-overlapping sub-trajectories, and the radar data are divided into corresponding sub-trajectories through time. In asynchronous calculation, the trajectory matching points are searched by the space-time constraint distance in each sub-trajectory segment to generate a set of candidate matching points. In the set of candidate matching points, the optimal trajectory matching point is searched, and the space-time distance of the optimal matching point is used as the basic unit for calculating the similarity. Then the method calculates the similarity of each trajectory segment asynchronously. In track matching, the overall similarity of the track is calculated according to each track segment, and the maximum similarity

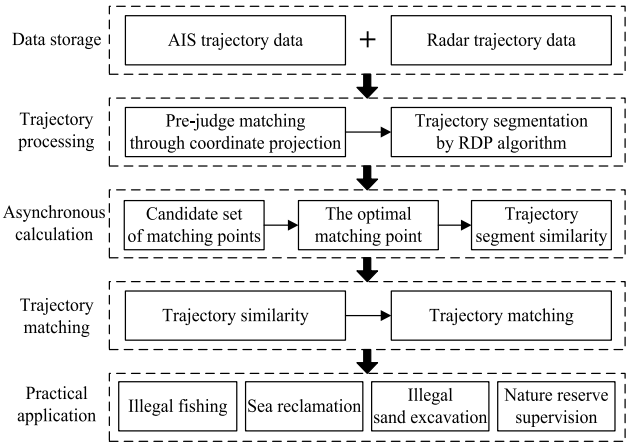

FIGURE 2. Framework of PTSCTM.

is used as the matching trajectory. The problem of AIS and radar trajectory matching is verified by the actual situation of AIS being artificially turned off. This method can be used in practical marine surveillance applications, such as illegal fishing, reclamation, illegal sand mining and monitoring of nature reserves. This article applies the method to the monitoring of the staying ships in the Qingdao lancelet reserve area.

The contents of each part are briefly described as follows: Section II mainly introduces the situation of the study area and explains the data used in the study. Section III elaborates on the related concepts of multi-source trajectory matching and defines the symbols to be used subsequently. Section IV describes the method of segmented trajectory matching in detail. In section V, the experiment is carried out according to the actual data and the performance of the segmented trajectory matching is verified with the comparison experiment. Section VI proposes a method for monitoring the staying ships in the Qingdao lancelet reserve area. Finally, this article is summarized.

II. RESEARCH DATA

The experimental data are AIS trajectory and shore-based radar trajectory data near Qingdao city, Shandong province, China on August 22, 2019. Fig. 3 shows the AIS and radar position data on August 22, 2019 in the study area. The data are stored in the ORACLE database in the form of relational tables.

A. AIS TRAJECTORY DATA

The AIS trajectory data used in this article is provided by the North China Sea Data & Information Service. There are 71743 points and 430 AIS trajectories in the study area on August 22, 2019. The AIS data interval is based on the actual upload time of the ship. AIS trajectory data contain dynamic information such as course, speed, position, and navigation status, as well as static information such as ship's name and call sign, International Maritime Organization (IMO)

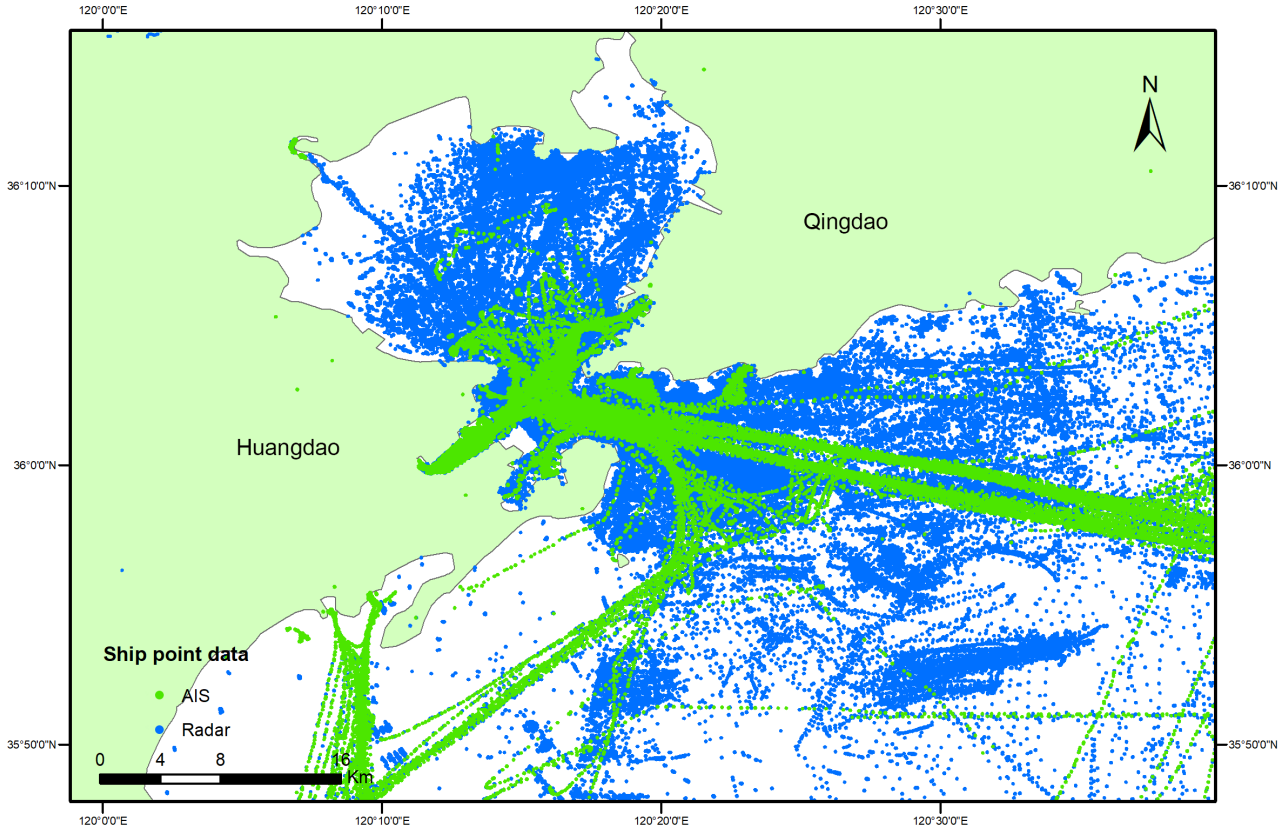

FIGURE 3. AIS and radar ship point data in the study area on August 22, 2019. The green point denotes the AIS trajectory point, and the blue denotes the shore-based radar trajectory point.

number, Maritime Mobile Service Identify (MMSI), type and antenna position.

B. SHORE-BASED RADAR TRAJECTORY DATA

Shore-based radar is usually responsible for sea and low-level surveillance and completes the tasks of searching, tracking, and navigating sea targets. The data used in this article is the shore-based radar trajectory data in the study area on August 22, 2019, from the North China Sea Data & Information Service. The shore-based radar trajectory data are returned every 4 minutes and the total amount of detection point data is 268,788. These data have been correlated at the sensor level. The shore-based radar data are used as radar trajectory data in this article. Due to the complexity of radar under multi-target tracking, a total of 62,163 trajectories are obtained. There are 57,861 trajectories with points below 0-10, accounting for 93%. As shown in Fig. 4, the number of points in the radar trajectory is more than 10. Considering the application of maritime supervision, trajectories with more than 30 points in each trajectory are selected in experimental data, for a total of 1,183 trajectories. Since radar data is returned every 4 minutes, the trajectory time of more than 30 points is more than 2 hours. This article believes that 2 hours is the minimum time that

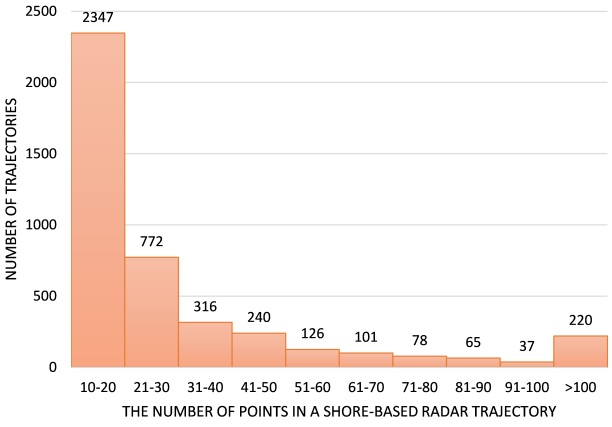

FIGURE 4. Statistic of the number of points in the shore-based radar trajectory.

can be used to discover the behavior of the ship. If trajectory time is less than 2 hours, it has little significance for trajectory matching and ship supervision. Radar trajectory data contain ID, longitude, latitude, speed, direction, and target length. ID is the unique identification of the radar trajectory.

III. INSTRUCTION OF MULTI-SOURCE TRAJECTORY MATCHING

A. DEFINITION OF MULTI-SOURCE TRAJECTORY

The trajectories generated in different systems have different signs and paths, which is affected by the working principle, processing mechanism and internal mode of different sensors [42]. At the same time, the trajectories affected by the sensor will have different noise and errors in different systems. The ship trajectory formed by multiple sensors for the same target becomes a multi-source trajectory The shape of the trajectory is different because the multi-source trajectory time is different and the location is different. As shown in Fig. 5, Tr is the detection trajectory of shore-based radar, and Ta is the report trajectory of AIS. Obviously, the trajectory data of different sensors are not uniform in time.

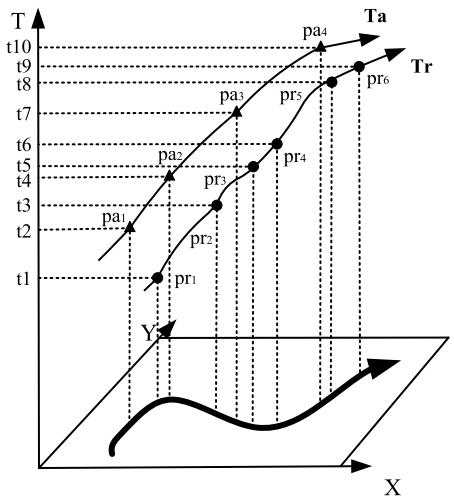

FIGURE 5. Schematic diagram of multi-source trajectory.

B. PRINCIPLE OF MULTI-SOURCE TRAJECTORY MATCHING

The time interpolation method isn't suitable for this situation due to the sampling uncertainties such as noise and data loss of multi-source trajectories. Multi-source trajectory points represent the data sampling points of two trajectories with the same motion behavior, and it is often impossible to record the same motion synchronously. The main idea of space-time constraints trajectory matching is to find as many "space-time matching points" on the trajectory as possible. Although the trajectory data may be affected by factors such as errors, delays, noise, and losses, the target measurement results from different sensors still have many associations [42]. Through space-time constraints, trajectory matching is to find a similar point between a trajectory and a related trajectory, use the similar point as a matching point and use the matching point as the minimum unit of similarity calculation. Only trajectory points satisfying the space-time distance can be regarded as approximate matching points. The matching point is within a certain time range and space range.

$$\begin{cases} spaceDis\left(pa_i, pr_j\right), & \left|pa_i, pr_j\right| \le \eta \\ timeDis\left(pa_i, pr_j\right), & \left\|pa_i, pr_j\right\| \le \varepsilon \end{cases} \tag{1}$$

where η represents the matching spatial distance of matching points, ε is the matching time distance. i is the ith point on Ta, and j is the jth point on Tr. $|*, *|$ is the spatial distance function of the trajectory points of different sensors, using Euclidean distance. $\|*, *\|$ is the time distance function of the trajectory points of different sensors, using the time difference.

As shown in Fig. 6, the point time on Tr and Ta is not synchronized. However, after passing the space-time constraint, the points within the constraint range can be regarded as matching points. pr_2 can match with pa_2, pr_3 can match with pa_3 and pa_4, pr_4 can match with pa_5 and pa_6. When a trajectory is matched with a trajectory, there will be multiple points that match this point within the space-time constraints. In the next chapter, this article will analyze and solve the problem.

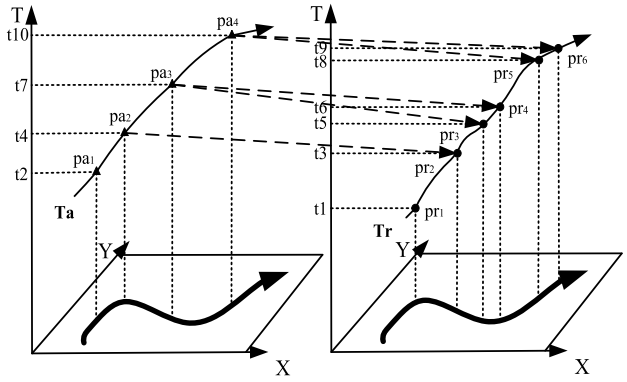

FIGURE 6. Multi-source trajectory matching.

C. DEFINITION OF SYMBOLS

Trajectory: A collection of data points located by sensors in chronological order. Since each trajectory is identified by a unique representation, AIS is identified by a MMSI code, and radar is identified by an ID code. AIS trajectory is written as: Ta = {pa | pa_i, $1 \leqslant i < m$, m is the number of AIS trajectory data points}, and the radar trajectory data are also written as: Tr = {pr | pr_j, $1 \leqslant j < n$, n is the number of radar trajectory data points}.

Trajectory segment: After passing through the segmentation process, the trajectory will be divided into a set of multiple trajectory segments. The original trajectory is written as Ta = {Sa | Sa_l, $1 \leqslant l < k$, k is the number of trajectory segments included in the AIS trajectory}, Sa_l = {pa | pa_q, $1 \leqslant q < s$, s is the number of points per trajectory segment }. After segmentation, the number of AIS and radar trajectory segments is the same, with Tr = {Sr | Sr_l, $1 \leqslant l < k$ }.

Candidate trajectory matching point set: Since there will be multiple points matching the AIS points within the space-time distance, the radar points matching the pai will be set to C_i $C_i = \{pr \mid pr_{i,p}, 1 \leqslant p < c, c$ is the number of matching sets$\}$.

Optimal trajectory matching point: pa_i and the point pr_i that has the closest space-time distance in the corresponding matching point set C_i are recorded as $[pa_i, pr_i]$. Matching points are the concept of pairs.

The symbols used later are defined in Table 1:

TABLE 1. Definition of symbols.

Name	Significance
Ta(Tr)	AIS trajectory (radar trajectory).
Sa(Sr)	Trajectory segment divided by AIS trajectory (trajectory segment divided by radar trajectory).
θ	Maximum distance of trajectory segment.
η	Space-constrained distance of trajectory matching point.
ε	Time-constrained distance of trajectory matching point.

IV. AN ASYNCHRONOUS TRAJECTORY MATCHING METHOD BASED ON PIECEWISE SPACE-TIME CONSTRAINTS

A. PRE-JUDGMENT OF SPACE-TIME PROJECTION

It is necessary to determine in advance whether the two trajectories match to avoid unnecessary calculations when the spatial range is large. Time overlap and spatial projection intersection are used to judge in advance. The time overlap judgment is to determine whether the trajectory matches by judging whether the time of the starting coordinates of Ta and Tr intersect. If Ta.st (the start time of Ta) is earlier than Tr.et (the end time Tr) and Tr.st (the start time of Tr) is later than Ta.et (the end time Ta), it means that Ta and Tr overlap in time.

$$Ta.st < Tr.et \;\&\&\; Tr.st < Ta.et \tag{2}$$

In the judgment of similar trajectory space, it is judged by whether the coordinate axis projections of Ta and Tr intersect. First, the projections of the trajectories of Ta and Tr on the X and Y coordinate axes are obtained. In the method, it is assumed that the projection of Ta on the X axis is X1 and the projection on the Y axis is Y1, corresponding to X2 and Y2. If X1 intersects X2 or Y1 intersects Y2, Ta and Tr may match. The projection X1 of Ta on the X axis and the projection X2 of Tr_1 on the X axis intersect, and there may be a common trajectory. The projection X2 of Ta on the X axis and the projection Y2 of the Y axis do not intersect with the projection X3 of Tr_2 on the X axis and the projection Y3 of the Y axis, indicating that Ta and Tr_2 will not match. Fig. 7 is a schematic diagram of the projection judgment.

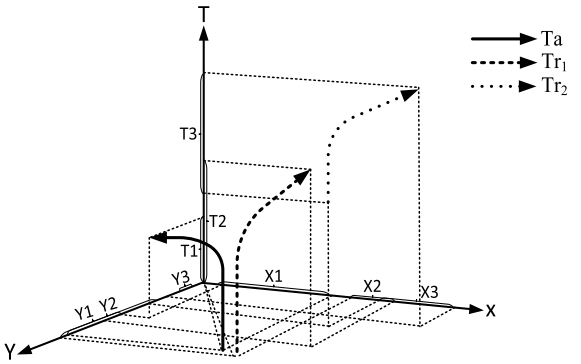

FIGURE 7. Pre-judgment by space-time projection.

B. DIVISION OF TRAJECTORY SEGMENTS

Because the traditional trajectory matching algorithm needs to perform space-time constraints on all points in the trajectory, the time complexity is o(mn). At the same time, the time and trajectory points increase, and the calculation time increases rapidly. In order to reduce the computational cost, this article uses the Ramer–Douglas–Peucker (RDP) trajectory compression algorithm to divide the original trajectories into sub-trajectories with shorter lengths and non-overlapping. The RDP algorithm was first proposed by Urs Ramer in 1972 [43]. Poiker and Douglas improved the algorithm in 1973 [44], and the algorithm then gradually was improved by many scholars. The RDP algorithm obtains an approximation of the original polygon by extracting the feature points of the polygon. It has been widely used in ship trajectory compression [45], [46].

The RDP algorithm uses recursive thinking. First, a distance threshold is set, and then a straight line is connected between the first point and the last point of the point set. The farthest point is found in the offline segment of the remaining points. If the distance between this point and the line segment is less than the threshold, all points in the middle are discarded. If it is larger than the threshold, the point is used as an intermediate point to generate two line segments with the first two points. The algorithm repeats the above process. The algorithm ends when all points are used. The trajectory matching algorithm performs trajectory point matching operations in sub-trajectories to reduce computational complexity and support the characteristics of online computing. The steps are as follows:

(1) The algorithm connects the starting point p_1 and the ending point p_2, and then calculates the distance from the remaining points to the line segment p_1p_2. The remaining points sequentially calculate the distance to the line segment p_1p_2, and obtain the maximum distance dmax. The point p_3 in Fig. 8a has the largest distance p_1p_2, and the distance is larger than the threshold θ. p_3 is connected with the starting points p_1 and p_2 to form a dotted line segment p_1p_3 and p_3p_2.

(2) When step (1) is performed on p_1p_3 and p_3p_2 respectively, p_4 is obtained. As shown in Fig. 8b;

(3) If dmax is not greater than θ, the algorithm ends. The final result is shown in Fig. 8c. p_1, p_3, p_5, p_4, p_2 are used as trajectory feature points.

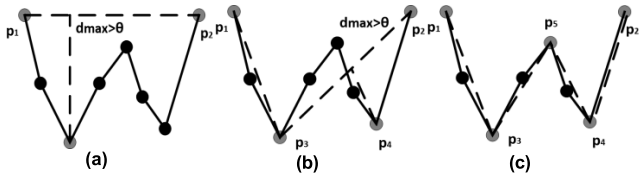

FIGURE 8. Schematic diagram of the RDP algorithm.

C. CALCULATION OF OPTIMAL MATCHING POINT

In the course of trajectory matching, multiple points that meet the time threshold and the space threshold will appear at the matching point of the space-time constraint. Points that meet the constraints of space-time constitute a set of matching points. The optimal matching point is proposed to calculate accuracy. By calculating the space-time distance of the points in the set, the point with the smallest distance is taken as the optimal space-time matching point. η is the space threshold, ε is the time threshold, pa_i is the point on the Ta trajectory, and C_i is the set of points matching the pa_i in time and space. The formula for calculating the optimal matching point $f(pa_i, pr_i)$ is defined as follows:

$$f(pa_i, pr_{i,p}) = \left(\frac{\eta - |pa_i, pr_{i,p}|}{\eta} * \frac{\varepsilon - \|pa_i, pr_{i,p}\|}{\varepsilon}\right) \quad (3)$$

where f(*,*) is the formula for calculating the space-time distance between the candidates of pa_i and pr_i. The value range is [0, 1]. The larger the value is, the closer the space-time distance is, indicating that the two points are closer. The space-time distance is inversely related to the result of f(*,*).

The largest result in $f(pa_i, pr_{i,p})$ is the optimal trajectory matching point. The optimal trajectory matching point indicates that the two matching points are closest in time and space. For the purpose of calculation, the spatial distance of the similarity calculation in the optimal matching point is used as the similarity calculation function. The calculation of the optimal matching point is as follows:

$$[pa_i, pr_i] = \max\{f\left(pa_i, pr_{i,1}\right), f\left(pa_i, pr_{i,2}\right), \ldots, f(pa_i, pr_{i,p})\} \quad (4)$$

where [pai, pri] is the optimal matching point pair, and max{*,*, . . . ,*} is the maximum value. p is the index in the set of candidate matching points of the trajectory point, $0 \leqslant p < c$. c is the number of the set of candidate matching points.

As shown in Fig. 9a, when the space-time constraints ε and η are satisfied, the point pa_1 in Ta matches pr_{21} in Tr_2, the point pa_2 in Ta matches pr_{22} and pr_{23} in Tr_2, the point pa_4 matches pr_{25} in Tr_2. Since $f(pa_2, pr_{22}) > f(pa_2, pr_{23})$, $[pa_2, pr_{22}]$ will be formed here as a matching point pair. In Fig. 9b, Ta and Tr_1 form a matching point $[pa_2, pr_{12}]$. Ta and Tr_2 form a total of 3 matching point pairs, $[pa_1, pr_{21}]$, $[pa_2, pr_{22}]$ and $[pa_4, pr_{25}]$.

D. CALCULATION OF TRAJECTORY SIMILARITY

On the basis of finding the optimal matching point, the similarity of the trajectory formed by two different sensors is calculated, and then the matching is determined. Due to the time threshold ε and the spatial threshold η, some points on Ta do not match the relevant points on Tr. In this article, the similarity calculation result of the points that Ta cannot match on Tr is 0, to meet the final calculation needs. The final similarity calculation formula for trajectory matching similarity is:

$$P_{score,i}\left([pa_i, pr_i]\right) = \begin{cases} 1 - \dfrac{|pa_i, pr_i|}{\eta}, & pri \neq NULL \\ 0, & pri = NULL \end{cases} \quad (5)$$

where [pa_i, pri] is the trajectory matching point pair, where $0 \leqslant i < m$, m is the number of AIS trajectory points. When pr_i = NULL, it means that pa_i of the current ith point cannot find a matching point on Tr under the time threshold $\boldsymbol{\varepsilon}$ and space threshold η. When $pr_i \neq$ NULL, pr_i is the best advantage of pa_i calculation, and the spatial distance is used as the basis of similarity calculation.

The calculation of the similarity between AIS and radar trajectory is composed by adding the similarity score $P_{score,i}$ $(0 \leqslant i < m)$ of each point. The formula for calculating the similarity between AIS and radar trajectories is as follows:

$$T_{score} = \frac{\sum_{i=0}^{m-1} P_{score,i}}{m} \quad (0 \leq i < m) \quad (6)$$

where T_{score} is the similarity score between AIS trajectory and radar trajectory, m is the number of AIS points. It indicates that the two trajectories are closer that the similarity score T_{score} of the trajectories is larger. Conversely, the lower the similarity score is, the farther the two trajectories are.

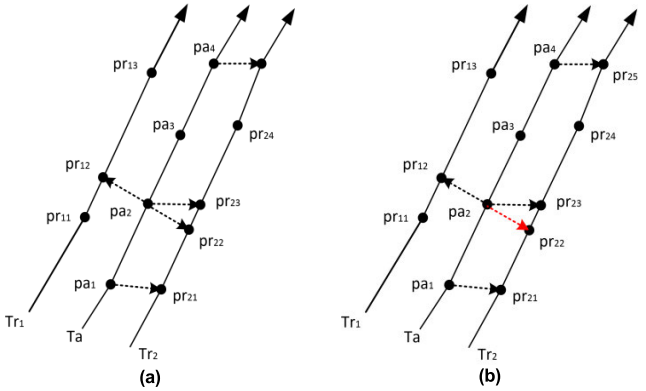

FIGURE 9. (a) is the selection of trajectory matching points; (b) is the selection of optimal matching points.

E. SIMILARITY CALCULATION AFTER SEGMENTATION

After calculating the similarity between trajectory matching points, it is necessary to calculate the similarity between trajectory segments divided by feature points. The similarity between the trajectory segments is determined by the degree of matching of the trajectory points within the segments. The point on Ta only matches the trajectory point on Tr in this segment to reduce the time of finding the matching point

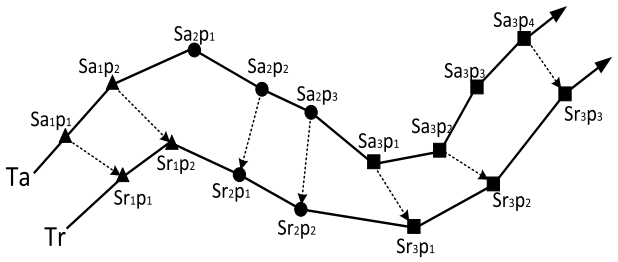

FIGURE 10. The best matching point is found based on piecewise space-time constraints.

after the trajectory is segmented. As shown in Fig. 10, after Ta is divided by the RDP algorithm, Ta is divided into {Sa_1, Sa_2, Sa_3}, and Tr is {Sr_1, Sr_2, Sr_3}. The points p_1 and p_2 on Sa_1 are searching for points on Sr_1, and cross-trajectory segment matching is not performed. When the point p_1 on Sa_2 is matched, the trajectory point can be matched on Sr_1, but not be matched on Sr_2. However, this article believes that these effects on the calculation results are slight in the long trajectory.

Therefore, the similarity of the trajectory segment is defined as the average value of each trajectory point in the trajectory segment. This can avoid large errors in individual jump points in the trajectory segment, and can also be used as a quantitative indication of trajectory segment matching. The formula for calculating the similarity of the trajectory segment is obtained:

$$S_{score,l} = \frac{1}{s} * \sum_{o=\mathrm{q}}^{s-1} P_{score,\mathrm{q}} \quad (0 \le q < s) \tag{7}$$

where $S_{score,l}$ represents the similarity score of the lth trajectory segment in the trajectory T. For $0 \leqslant q < s$, q is the index of the trajectory point in the trajectory segment. s is the number of trajectory matching points of the trajectory segment.

In the case of calculating the overall score of the trajectory segment, the calculation formula of the similarity score of the trajectory is modified to the average value of the similarity score of each trajectory segment. The calculation is as follows:

$$T_{score} = \frac{\sum_{l=0}^{k-1} S_{score,l}}{\mathrm{k}} \quad (0 \le l < k) \tag{8}$$

where T_{score} is the similarity score of AIS trajectory and radar trajectory. k is the number of divided trajectory segments. l is the divided lth trajectory, where $0 \leqslant l < k$.

F. ASYNCHRONOUS TRAJECTORY MATCHING PROCESS

After calculating the similarity between AIS and radar trajectories, the possibility of two trajectories being the same trajectory can be quantitatively evaluated through the similarity between trajectories. This evaluation method can be used in trajectory matching and association. TA and TR are the set of target trajectories generated by AIS and radar respectively. $Ta_i \in TA$ and $Tr_j \in TR$ respectively represent the ith AIS trajectory and the jth radar trajectory. The algorithm steps are as follows:

(1) The algorithm first traverses $tr_j \in TR$ in the radar set and judges whether the projections of Ta_i and Tr_j intersect $Ta_i \cap Tr_j$ in time and space. If they intersect, the algorithm goes to the next step. If they do not intersect, the algorithm exits.
(2) The AIS trajectory Ta_i uses the RDP algorithm to extract feature points and is divided into segments through the feature point. At the same time, the radar trajectory Tr_j is also segmented according to time.
(3) In each trajectory segment, matching points are found resulting in candidate point combinations through time constraints and space constraints. The optimal matching point is calculated through the space-time distance. In each trajectory segment, matching points are founded asynchronously resulting in candidate point combinations through time constraints and space constraints. The optimal matching point is calculated through the space-time distance. The similarity score pairs of each matching point are summed, and the average value is used as the similarity of each trajectory segment.
(4) The similarity of each trajectory segment is summed, and the average value is calculated as the similarity score of the trajectory. The highest score is the trajectory associated with Ta_i and Tr_j matching.

V. EXPERIMENT ANALYSIS

A. TRAJECTORY MATCHING WHEN AIS IS TURNED OFF

After judging the intersection of time and space, the multi-source trajectory similarity is calculated for the intersecting AIS trajectory and radar trajectory. In the following experiment, the AIS trajectory whose MMSI is 413330760 and the radar trajectory whose ID is 6569939253935038464 are used to conduct the trajectory matching experiment when the AIS is turned off. The name of the ship whose MMSI is 413330760 is "TONG BAO 2". The minimum interval of AIS adjacent trajectory points is 16s, and the maximum interval is 11 hours and 38 minutes. The ship is located near the Qingdao Sea, as shown in Fig. 11a. The AIS trajectory is segmented by RDP, where the distance threshold θ of the segment is set to 200m, and feature points are extracted. The AIS trajectory extracts 14 feature points, divides the trajectory into 13 trajectory segments, and also has a corresponding radar trajectory. As shown in Fig. 11b.

After the trajectory segment is divided, the matching point of the trajectory is calculated by the definition of multi-source trajectory matching. The space constraint distance η is 500m, and the time constraint distance ε is 4 minutes. When $\eta =$ 500m and $\varepsilon =$ 4min, the matching point is calculated from each point in the AIS trajectory, and the optimal matching point is calculated by the optimal matching point calculation function. Through the similarity of matching points, the

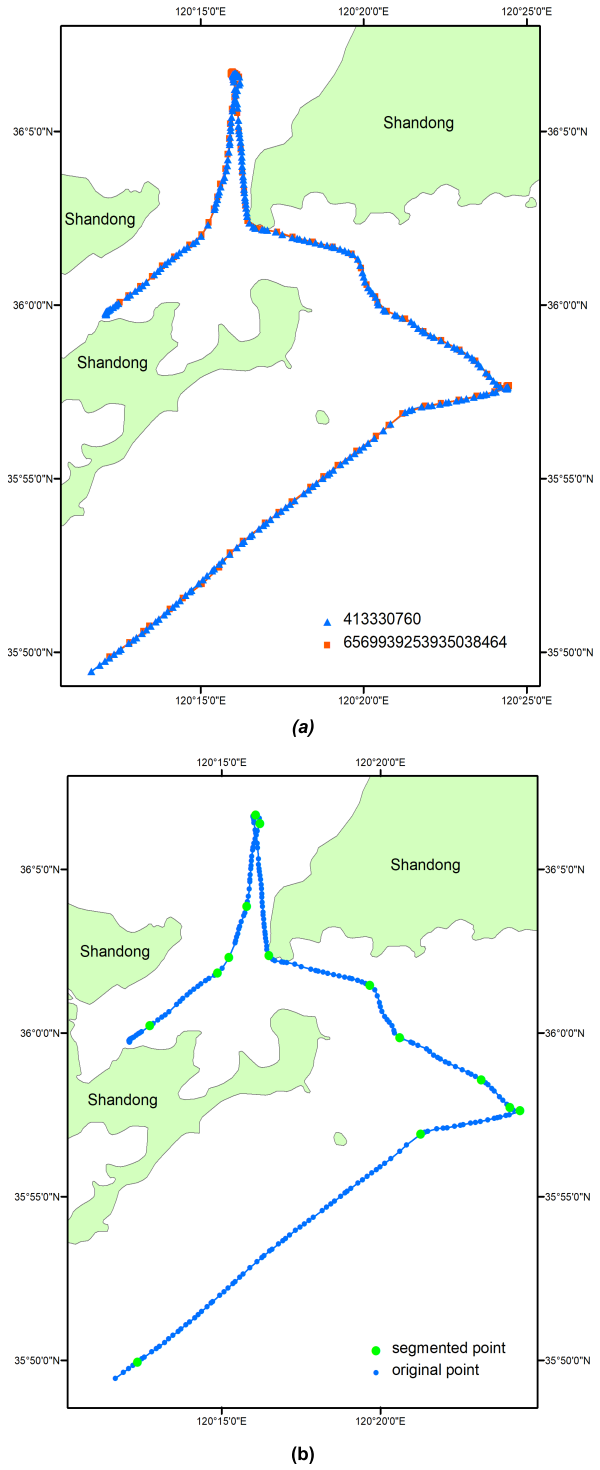

FIGURE 11. (a) is the ship's trajectory data: The AIS trajectory with MMSI of 413330760 and the radar trajectory with ID of 6569939253935038464; (b) is the result of using RDP to divide AIS trajectory.

similarity in the trajectory segment is calculated, and finally, the similarity of the two trajectories is calculated. When the time interval is 4min, most of the points can find matching points, and then the optimal matching point is calculated from the set of candidate matching points. There are also some

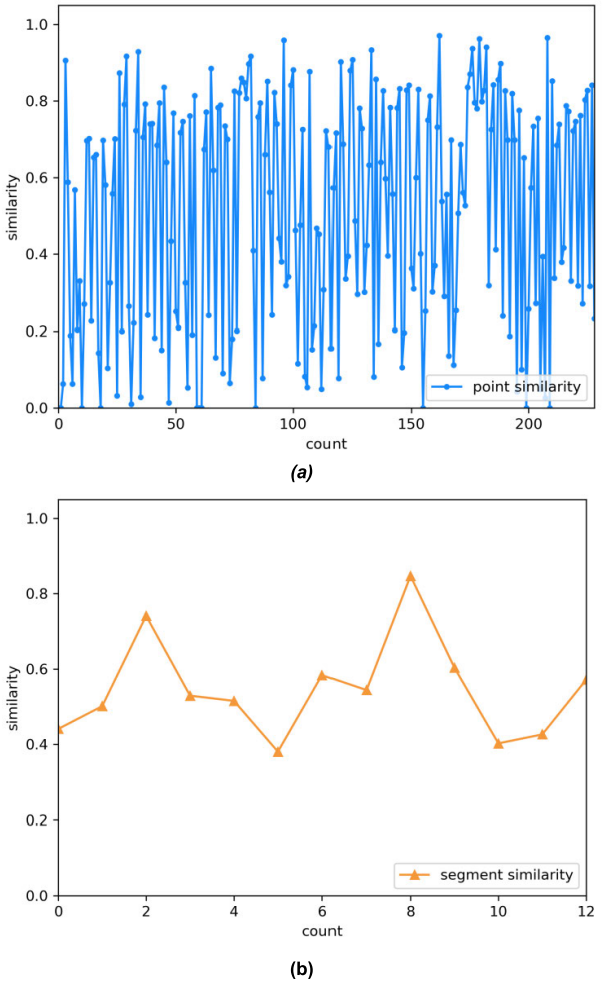

FIGURE 12. (a) is The similarity of points of the optimal matching point; The average similarity within the trajectory segment.

points that cannot be matched under the constraints of time and space, and the value of these points is 0. Fig. 12a is the similarity of points of the optimal matching point. Then the similarity of each segment is calculated and many matching points are found. This means that the trajectory of the same target from different sensors will match more points within the constraints of time and space. Fig. 12b is the average similarity within the trajectory segment after the trajectory is segmented according to RDP. Table 2 shows the calculated similarity for each trajectory segment.

B. ANALYSIS OF SPECIFIC TRAJECTORY ROUTES

This section discusses in detail when AIS is turned off. After completing the AIS trajectory and radar trajectory segment trajectory matching, it is found that AIS has been turned off for a long time. As shown in Fig. 14, the AIS trajectory whose MMSI is 413330760 has a long period of closure from 2019-8-22 03:18:30 to 2019-8-22 08:45:33 and from 2019-8-10:34:43 to 2019-8-22 22:13:06. However, the radar trajectory whose ID is 6563939253935038464 can still

TABLE 2. Similarity for each trajectory segment.

Trajectory segment	Start and end time	Similarity
first segment	01:44:33 ~ 02:46:22	0.44073
second segment	02:49:31 ~ 03:14:24	0.50112
third segment	03:15:30 ~ 08:45:33	0.74098
fifth segment	08:56:14 ~ 09:15:23	0.51518
sixth segment	09:15:52 ~ 09:33:05	0.38035
eighth segment	09:58:26 ~ 22:15:33	0.54390
ninth segment	22:16:02 ~ 22:17:54	0.84715
tenth segment	22:19:44 ~ 22:37:20	0.60322
eleventh segment	22:38:19 ~ 22:47:14	0.40236
twelfth segment	22:50:34 ~ 22:53:03	0.42616
thirteenth segment	22:54:28 ~ 23:12:14	0.57146

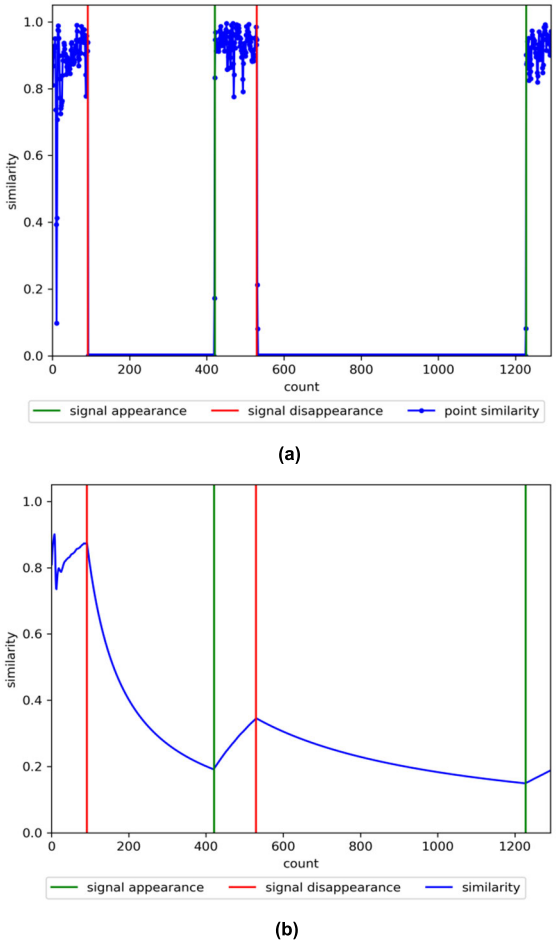

FIGURE 13. (a) is the point similarity of the time interpolation method; (b) is the cumulative similarity of the trajectory by the time interpolation method.

maintain signal collection when the AIS is turned off, and it can completely record the actual route of the ship.

VI. EXPERIMENTAL COMPARISION

A. COMPARISON WITH TIME INTERPOLATION

The AIS trajectory whose MMSI is 413330760 and the radar trajectory whose ID is 6569339253935038464 are also used for comparison and explanation with the traditional time interpolation method. The point similarity after time interpolation using the same spatial threshold is restored under the same conditions. When the AIS is turned off, the similarity slowly decreases to 0, and then when the AIS is turned on, the similarity returns to the normal range, as shown in Fig. 13a. When the time is from 2019-8-22 03:18:30 to 2019-8-22 08:45:33, from 2019-8-22 10:34:43 to 2019-8-22 22:13:06, the AIS report disappears. As a result, it is impossible to match with the radar, and a large number of point similarities are 0. As shown in Fig. 13b, the loss of the AIS trajectory results in a far deviation from the radar trajectory, and the calculated similarity is very slight, so trajectory matching cannot be performed. When using the idea of matching points at that time, this method avoids time interpolation and only matches the points on the trajectory, effectively avoiding interpolation errors and missing points, which leads to erroneous calculations.

B. TRAJECTORY MATCHING ACCURACY VERIFICATION

In order to verify the accuracy of the algorithm, 12 AIS trajectories and 13 radar trajectories are adopted in the dense environment. Through the time interpolation method and the proposed algorithm in this article respectively, the matching results of radar and AIS trajectory are compared. As shown in Fig. 15, there is a situation that the AIS is turned off in the trajectory.

The calculation formula for the accuracy of the matching result is defined:

$$\rho = \frac{\gamma_0}{\gamma} \times 100\%$$

where $\boldsymbol{\rho}$ represents the accuracy of matching, $\boldsymbol{\gamma}$ is the number of AIS tracks in the experiment, and $\boldsymbol{\gamma_0}$ is the number of correct matches. The matching result is compared with the matching result of long-term observation. The larger the $\boldsymbol{\gamma_0}$ value, the more correct matching trajectories and the higher the accuracy.

As shown in Fig. 16, a is the matching result of the time interpolation method, and b is the matching result of the proposed algorithm in this article, and different colors are marked according to different matching results. Matching results belonging to a ship are represented by the same color.

Based on the time interpolation method, the AIS trajectory matches the adjacent radar trajectory when the AIS is turned off. However, long-distance tracking found that this is not correct. The accuracy of this method is $\boldsymbol{\rho = \frac{10}{12} \times 100\% \approx 83.3\%}$. Through the proposed algorithm in this article, it is found that when AIS is turned off, the AIS trajectory can still match the correct radar trajectory. When the AIS is not lost, the accuracy of AIS and radar trajectory matching is still high. The accuracy of this method is $\boldsymbol{\rho = \frac{11}{12} \times 100\% \approx 91.6\%}$. From the analysis of the above results, it can be seen that the proposed algorithm in this article has good matching accuracy when the AIS is closed and not closed. Under the same parameters, comparing the

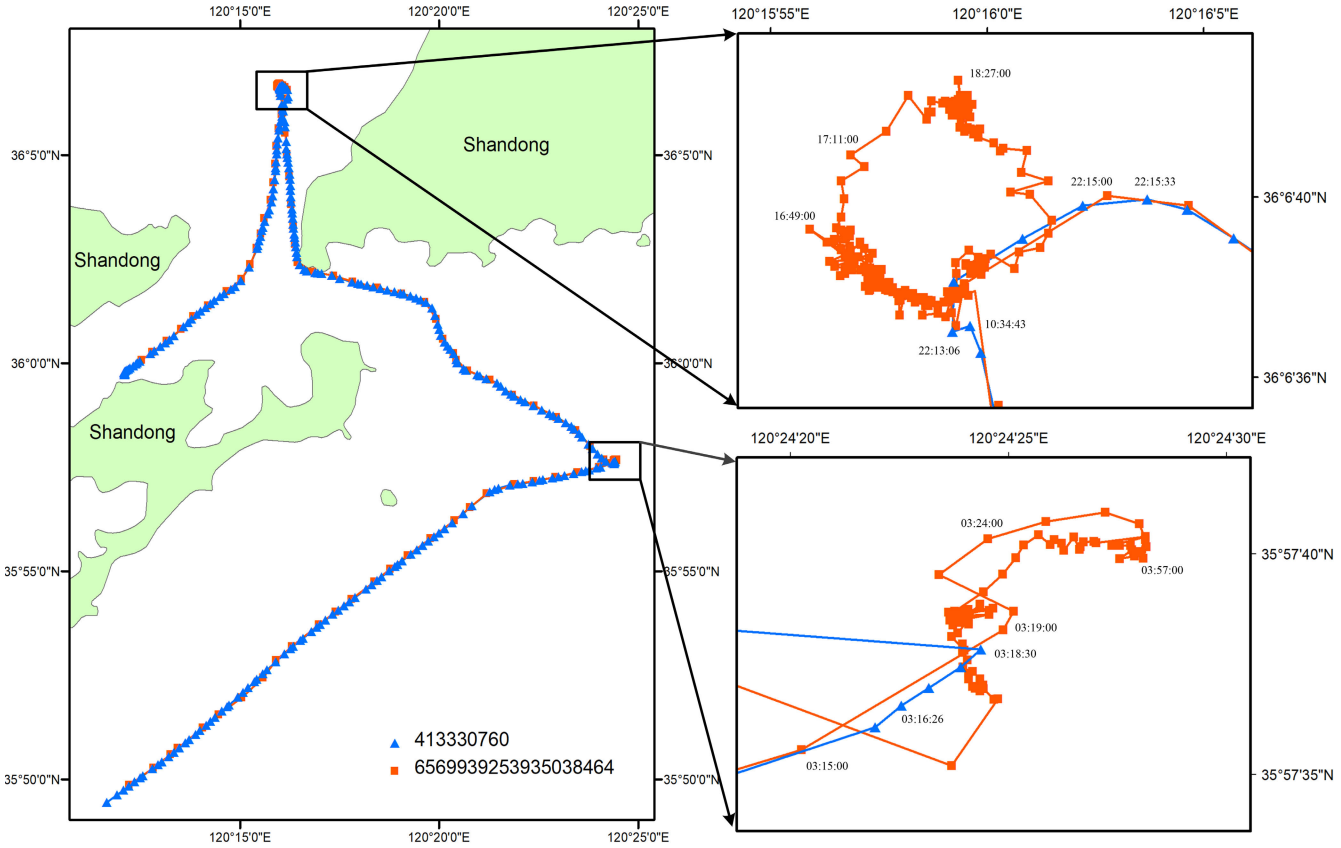

FIGURE 14. The detailed route of the ship whose AIS is turned off.

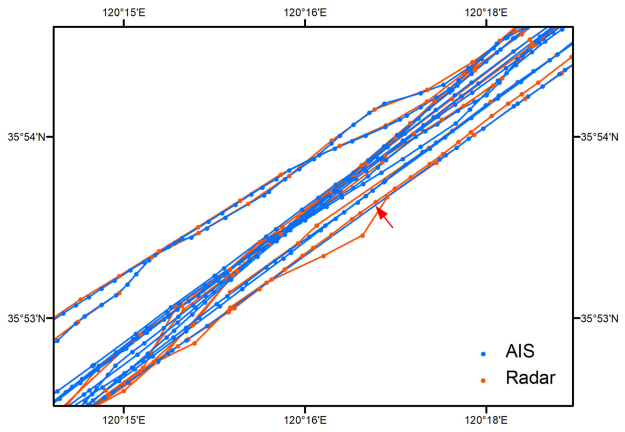

FIGURE 15. Trajectory data in accuracy verification. The red arrow points to the closed AIS trajectory.

TABLE 3. Comparison of parameter and accuracy of the two algorithms.

Algorithm	η	ε	Accuracy
Time interpolation	500m	/	83.3%
PTSCTM	500m	4min	91.6%

TABLE 4. Comparison of algorithm efficiency.

Algorithm \ Count (Time(ms))	229	644	1288	2575
PSTCTS	36.17	108.86	167.53	339.61
STCTS	29.06	96.96	180.61	446.58
DTW	194.74	599.82	901.10	2093.88
LCSS	210.53	436.37	850.52	2628.99
MHD	387.55	815.64	1971.0	3356.60

accuracy of time interpolation methods, the algorithm in this article has higher accuracy. The specific parameter settings and algorithm results are shown in Table 3 below.

C. COMPARISON WITH CALCULATING TIME

The experiment runs on a desktop computer. The operating system is Windows10, the CPU is A10-7300 and the memory is 8G. All algorithms are written in Java language, Java Development Kit (JDK) version is 1.8 and the software environment is IntelliJ IDEA 2019.3.4. The experimental data use the AIS trajectory whose MMSI is 413330760 and the radar trajectory whose ID is 6563939253935038464 in section V for experiments. The comparison experiment selects four measurement models: MHD, DTW, LCSS, and STCTS. The experiment takes the distance threshold $\eta = 500$m and the time threshold $\varepsilon = 4$min. The experiment takes the average time of 100 identical experiments to count the running time

TABLE 5. Illegal ships information.

MMSI	ID	Name	Type	IMO
413369020	6569945572767260672	NAN LIAN 16	oil tanker	9592161
413330760	6569939253935038464	TONG BAO 2	cargo ship	
413271610	6569760058806198272	TANGSHANCHANGSHENG 3	cargo ship	
413698660	6570161706825244672	HONG DA XIN 22	cargo ship	134234112
412330570	6569922933860425728	JIN FENG 3	cargo ship	524424
241664000	6569889320267767808	MARAN ARIES	oil tanker	9295000
413381040	6569846181465251840	HE ZHONG 5	oil tanker	9722259
413506090	6569760124153454592	XINHONGXIANG 89	cargo ship	16793600
412330070	6569931833108160512	TONG QING 6	cargo ship	
413216280	6570124863719170048	XING FA988	cargo ship	
413699020	6569856146116534272	XIN HONG XIANG 97	cargo ship	

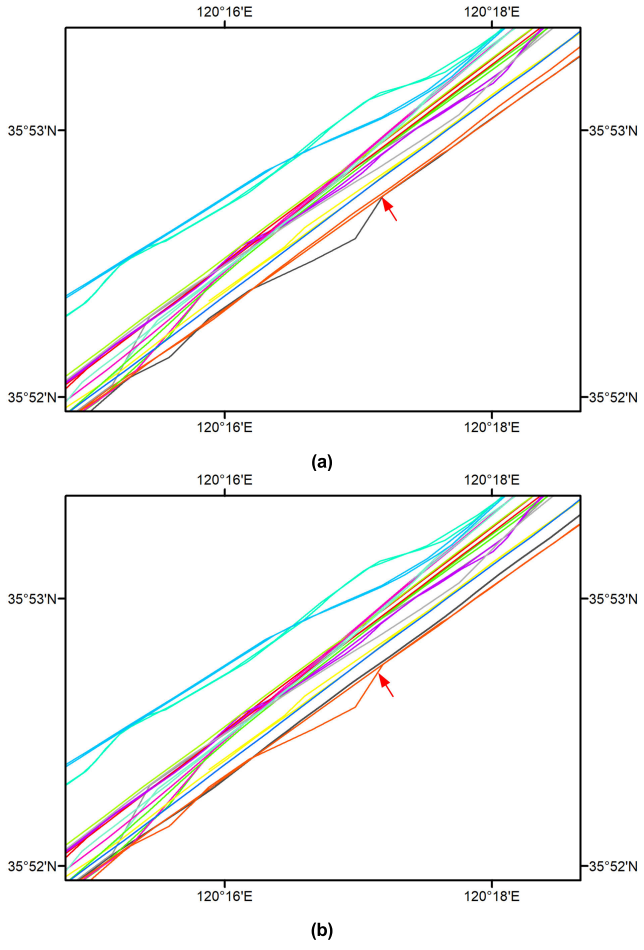

FIGURE 16. (a) is the matching result of the time interpolation method, and (b) is the matching result of PTSCTM.

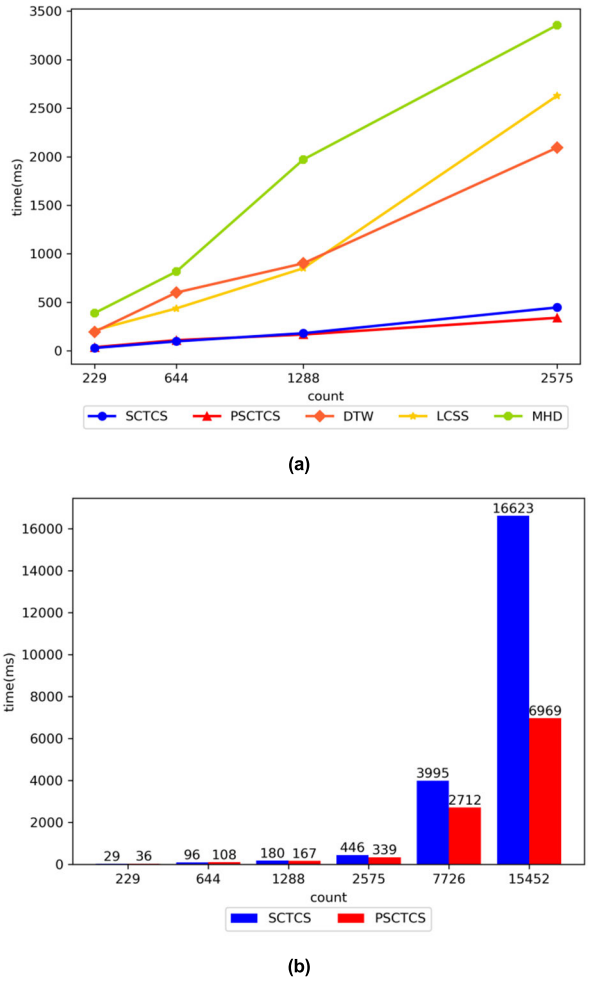

FIGURE 17. (a) is the running time of each algorithm; (b) is the running time comparison of SCTCS and PTSCTS.

of the program. As shown in Fig. 17a, it is found that the trajectory matching method based on space-time constraints is more time-efficient than the methods of LCSS, DTW, and MHD. Table 4 shows the detailed time of each method under different point data volume. At the same time, the performance of PTSCTS and SCTCS is compared for data under different data volumes, as shown in Fig. 17b. When the amount of data is small, the calculation time of SCTCS is less than that of PSCTCS. However, the calculation time

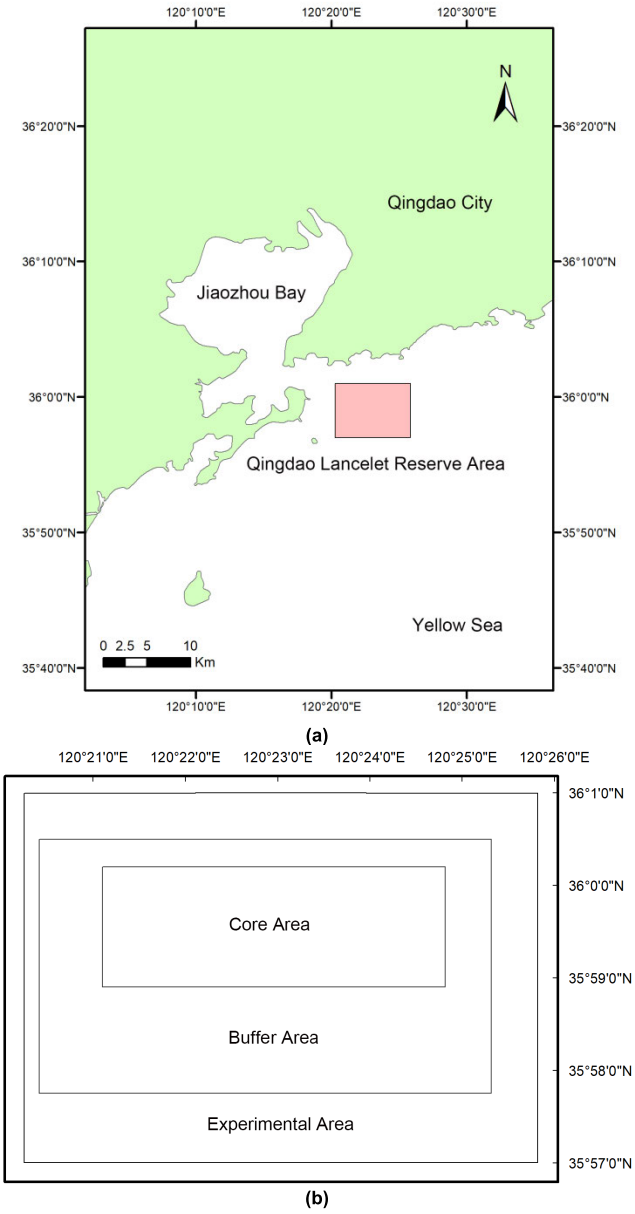

FIGURE 18. (a) is the location of the Qingdao lancelet reserve area; (b) is the internal division of the area.

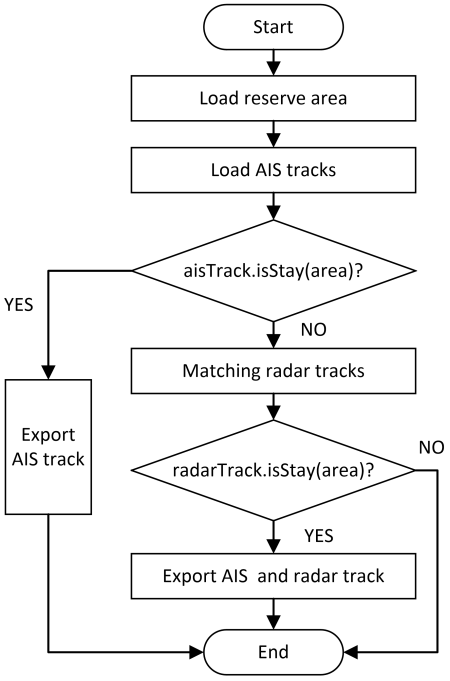

FIGURE 19. This is the step of the monitoring of the ship's stay.

of using PTSCTS is less than that of SCTCS as the amount of data increases. This is because it should take a long time for points on the AIS to perform a matching calculation on each point on the radar trajectory and calculate the optimal matching point. However, after RDP segmentation, the points on the AIS trajectory only need to find the matching point on the trajectory segment, and then the optimal matching point is calculated, which reduces the amount of global search data and guarantees the calculation time.

VII. PRACTICAL APPLICATION

A. INTRODUCTION OF MONITORING AREA

In the above method, the AIS trajectory matches the corresponding radar trajectory. The method can find the movement trajectory and achieve good results when closing the AIS trajectory for a long time. This article applies this method to the monitoring of the Qingdao lancelet reserve area. As shown in Fig. 18a, the Qingdao lancelet reserve area is located in 61.85 square kilometers of sea area outside the mouth of Jiaozhou Bay, northeast of Zhucha Island, and east of Daqiao Island. The tides and ridges formed on the seabed are rich in basic feed and are the best habitat for amphioxus. But the habitat of amphioxus has been destroyed in recent years for the phenomenon of excessive sea sand mining in this sea area. The Qingdao lancelet reserve area is specially established aiming at saving and restoring amphioxus in the Qingdao waters. As shown in Fig. 18b, the nature reserves are divided into core area, buffer zone and test area for the needs of natural environment, resource conditions and protection management.

B. STEP OF THE MONITORING OF SHIP'S STAY

It is conducive to discovering the ship's stay in the nature reserves and illegal or criminal acts at sea by monitoring the status of ships. The conditions for ships to stay in the nature reserves are first defined. Because trajectory points of the ship aren't only defined by the speed of trajectory points, but also by the speed characteristics and time characteristics of the trajectory points [47]. A ship that stays in a certain area has usually a much lower travel speed in the area than the speed outside the range, and the ship stays in the area for a certain period of time. In this article, the average speed of the ship's trajectory is used as a limiting condition. If the ship's speed in the area is lower than the average speed of the ship and the stay time exceeds the set minimum stay time threshold

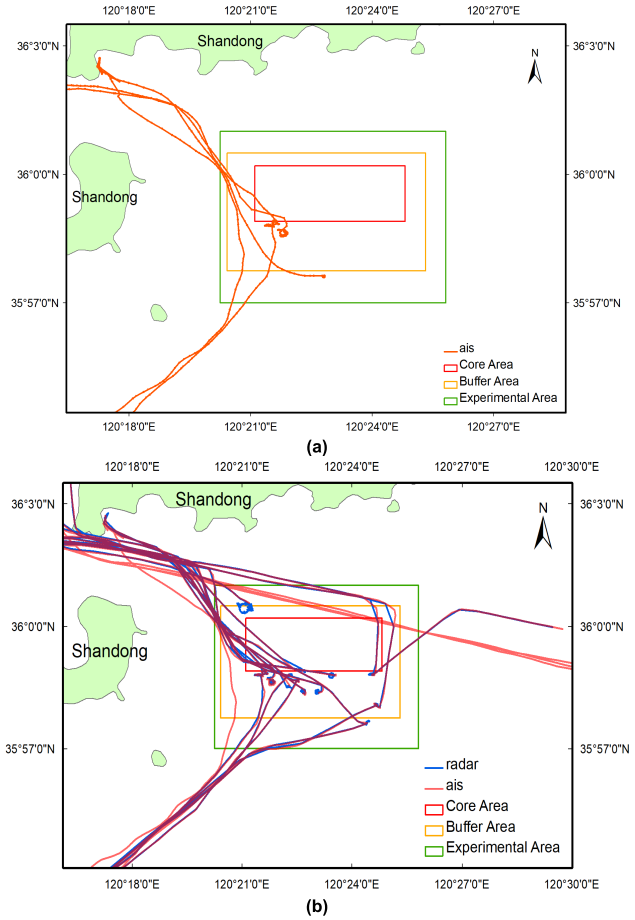

FIGURE 20. (a) is stay trajectories judged only by AIS reports; (b) is stay trajectories judged by the radar trajectory matched by AIS.

ST, it is considered that the ship has stopped in the area. The specific steps are shown in Fig. 19.

(1) Loading the Qingdao lancelet reserve area data and AIS report data;
(2) If the AIS trajectory data satisfy the conditions of stay in the nature reserve, the trajectory is considered to stay in the area and exported;
(3) If the AIS trajectory do not stay in this area, the algorithm loads the radar data to find the matching radar trajectory;
(4) If the matching radar data stay in the nature reserve, the AIS trajectory and the radar trajectory are exported. Otherwise, the algorithm ends.

C. RESULTS

First, the AIS trajectory is used for the monitoring of ship's stay. As shown in Fig. 20a, four trajectories will be found to stay in the nature reserve when only using the AIS trajectory data to determine the stay. The MMSI is 412925000, 413207320, 413491230, and 413368430 respectively. Then, AIS trajectory data that do not meet the monitoring conditions for the stay of the nature reserve is matched with

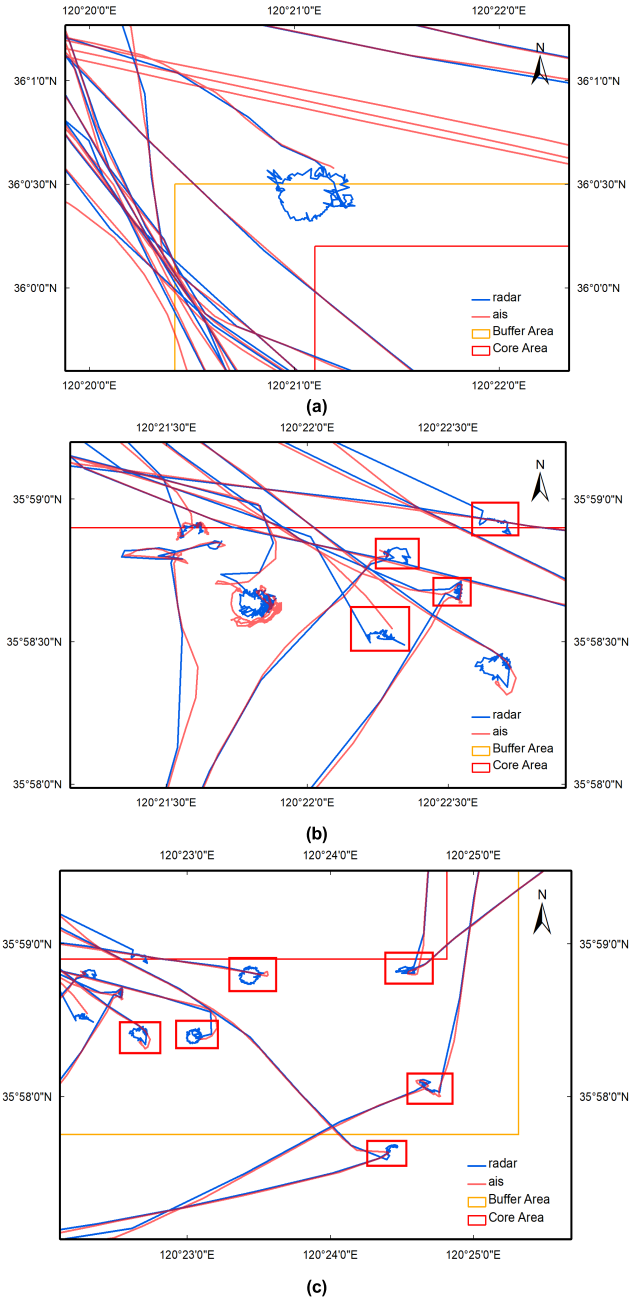

FIGURE 21. The radar trajectories were found to stay in the area, but the AIS trajectories were not found.

the radar trajectory. Then the corresponding radar trajectory is monitored. Several ships are found staying in the area. As shown in Fig. 20b, a large number of ships staying in the area are found. The straight trajectory at the upper right in Fig. 20b is trajectories recorded by AIS at other times.

In Fig. 21, the radar trajectory matching with the AIS trajectory appears to stay in the nature reserve. It is found that several ships turned off the AIS in the nature reserve, including an anchored state. When AIS is turned off in the nature reserve, the maritime supervisors cannot find their stay status and their actions The radar trajectory matching with the

AIS trajectory determines the ship's stay in the nature reserve with the advantages of active radar detection, and it will be found that there are a large number of ships when AIS is turned off in the nature reserve. However, AIS has identity information such as the ship's name, MMSI and IMO, etc. The maritime supervision department can easily find related ships. If the AIS trajectory data are only used to supervise the nature reserve, it will not be found that ships have stayed in the nature reserve. When AIS trajectory and radar trajectory are matched, the stay monitoring through the matched radar trajectory will find that many ships turn off their AIS in this nature reserve. AIS and radar signals complement each other to discover the staying behavior of ships in the nature reserves.

In Table 5, the information of ships that haven't found staying through the AIS trajectory but found staying through the matching radar trajectory is given to the Qingdao lancelet reserve area. In the table, MMSI is the MMSI number of the AIS trajectory, ID is the unique identifier of the radar trajectory matched by the AIS trajectory, Name is the name of the ship recorded by the corresponding AIS system, Type is the type of ship recorded by the AIS system, and the IMO number is the International Maritime Organization registered number. Since some ships only travel in China and haven't registered IMO, the IMO number is empty.

VIII. CONCLUSION

This article proposes the asynchronous trajectory matching method of AIS trajectory and radar trajectory based on piecewise spatial and temporal constraints, and the method is analyzed in detail. The radar trajectory data are used to distinguish trajectories of ships where AIS is turned off to discover the illegal driving activities of ships at sea. The main contributions of this article are as follows.

(1) This article introduces the problems faced by the maritime department after AIS is turned off and discusses the necessity of radar as a supplement to the AIS and the complementarity of radar trajectories.
(2) The calculation method of the optimal matching point is proposed. The optimal trajectory matching point is found in the set of candidate matching points with time and space distance based on spatial and temporal constraints, and it is used in the similarity calculation of trajectory matching.
(3) A trajectory matching algorithm based on piecewise spatial and temporal constraints is designed. The algorithm uses RDP to segment the trajectory and calculates the optimal matching point in the trajectory segment. Then it calculates the similarity of each trajectory segment asynchronously and the similarity of the trajectory. The AIS and radar trajectory with maximum similarity are matched trajectories. The trajectory matching algorithm proposed in this article has a higher accuracy and efficiency compared with the traditional way.
(4) This method is applied to the monitoring of the ship's stay in the Qingdao lancelet reserve area. It is found that a large number of ships stayed in the nature reserve by matching the radar trajectory when AIS is turned off. It can provide decision support for the maritime department to monitor the Qingdao lancelet reserve area.

The asynchronous trajectory matching method based on piecewise spatial and temporal constraints is used to match the AIS trajectory with the radar trajectory. The radar trajectory can effectively discover the ship's driving behavior when AIS is turned off. At the same time, AIS provides a ship identification method that can realize long-term tracking and monitoring of ships. This method is conducive to strengthening the supervision of marine ships and providing decision support to the maritime supervision department.

In future work, we will further study the method of asynchronous trajectory matching. (1) The ship's speed and angle and other characteristics will be taken as a part to the similarity calculation apart from the ship's positional relationship; (2) As the study area expands and the amount of trajectory data increases, the distributed trajectory matching method based on MapReduce will continue to be studied.

ACKNOWLEDGMENT

The authors would like to acknowledge the State Oceanic Administration of China for providing AIS and shore-based radar trajectory data.

REFERENCES

[1] A. K. Kuhn, "The international convention for safety of life at sea," *Amer. J. Int. Law*, vol. 31, no. 3, pp. 105–137, Jul. 1937.
[2] R. K. Appleyard, "Commission of the European communities," *Sci. Total Environ.*, vol. 85, pp. 10–12, Sep. 1985.
[3] H. Li, J. Liu, Z. Yang, R. W. Liu, K. Wu, and Y. Wan, "Adaptively constrained dynamic time warping for time series classification and clustering," *Inf. Sci.*, vol. 534, pp. 97–116, Sep. 2020.
[4] H. Li, J. Liu, K. Wu, Z. Yang, R. W. Liu, and N. Xiong, "Spatio-temporal vessel trajectory clustering based on data mapping and density," *IEEE Access*, vol. 6, pp. 58939–58954, 2018.
[5] L. Li, W. Lu, J. Niu, J. Liu, and D. Liu, "Fuzzy optimization model of high risk navigational area based on AIS data," in *Proc. 36th Chin. Control Conf. (CCC)*, Dalian, China, Jul. 2017, pp. 9977–9982.
[6] R. J. Bye and A. L. Aalberg, "Maritime navigation accidents and risk indicators: An exploratory statistical analysis using AIS data and accident reports," *Rel. Eng. Syst. Saf.*, vol. 176, pp. 174–186, Aug. 2018.
[7] D. Chen, N. Zhao, J. Lang, Y. Zhou, X. Wang, Y. Li, Y. Zhao, and X. Guo, "Contribution of ship emissions to the concentration of PM2. 5: A comprehensive study using AIS data and WRF/Chem model in Bohai Rim Region, China," *Sci. Total Environ.*, vols. 610–611, pp. 1476–1486, Jan. 2018.
[8] B. Ai, B. Li, S. Gao, J. Xu, and H. Shang, "An intelligent decision algorithm for the generation of maritime search and rescue emergency response plans," *IEEE Access*, vol. 7, pp. 155835–155850, 2019.
[9] Ministry of Transport of the People's Republic of China. (Mar. 9, 2018). *Special Rectification of National Maritime Radio Order Management*. [Online]. Available: https://mp.weixin.qq.com/s/EnDjsgLc06m3lxRtrv8IDw
[10] Y. Bar-Shalom, "On the track-to-track correlation problem," *IEEE Trans. Autom. Control*, vol. AC-26, no. 2, pp. 571–572, Apr. 1981.
[11] C. Lin, H. Lin, L. Li, J. Zhou, and Y. Ou, "Development of the integrated target information system of the marine radar and AIS based on ECDIS," in *Proc. 5th Int. Conf. Wireless Commun., Netw. Mobile Comput.*, Beijing, China, Sep. 2009, pp. 1–4.

[12] R. A. Singer and A. J. Kanyuck, "Computer control of multiple site track correlation," *Automatica*, vol. 7, no. 4, pp. 455–463, Jul. 1971.
[13] Y. He, Q. Tan, and R. Jiang, "Trajectory correlation algorithm in multi-sensory fusion system," *Fire Control Command Control*, vol. 14, no. 1, pp. 1–12, 1989.
[14] Y. He, D. Lu, and Y. Peng, "New track correlation algorithm for multitarget and multisensor tracking," *J. Tsinghua Univ., Sci. Technol.*, vol. 37, no. 9, pp. 108–113, Sep. 1997.
[15] Y. He, Y. Peng, D. Lu, and Z. Gao, "Binary track correlation algorithms in a distributed multisensor data fusion system," *J. Electron.*, vol. 19, no. 6, pp. 721–728, Nov. 1997.
[16] Y. He, D. Lu, Y. Peng, and Z. Gao, "Two new track correlation algorithms in a multisensor data fusion system," *Acta Electron. Sinica*, vol. 25, no. 9, pp. 10–14, Sep. 1997.
[17] Y. Chen, X. Si, and W. Li, "Research on data correlation based on fussy similarity," *J. Projectiles, Rockets, Missiles Guid.*, vol. 27, no. 2, pp. 385–388, Feb. 2007.
[18] Y. Ou, C. Lin, J. Zhou, and G. Chen, "Study on the target association arithmetic of the marine radar and AIS," in *Proc. 9th Int. Conf. Electron. Meas. Instrum.*, Beijing, China, Aug. 2009, pp. 3–815.
[19] Q. Guo and F. Zheng, "Track correlation algorithm based on likehood of topology," *Ship Electron. Eng.*, vol. 32, no. 9, pp. 43–45, Sep. 2012.
[20] Y. Mao, D. Zhang, and L. Wang, "A track association approach based on topoiogicai triangie simiiarity degree," *J. Equip. Acad.*, vol. 27, no. 4, pp. 69–74, Aug. 2016.
[21] H. Alt and M. Godau, "Computing the Fréchet distance between two polygonal curves," *Int. J. Comput. Geometry Appl.*, vol. 5, nos. 1–2, pp. 75–91, Mar. 1995.
[22] D. P. Huttenlocher, G. A. Klanderman, and W. J. Rucklidge, "Comparing images using the Hausdorff distance," *IEEE Trans. Pattern Anal. Mach. Intell.*, vol. 15, no. 9, pp. 850–863, Sep. 1993.
[23] J.-G. Lee, J. Han, and K.-Y. Whang, "Trajectory clustering: A partition-and-group framework," in *Proc. ACM SIGMOD Int. Conf. Manage. Data (SIGMOD)*, Beijing, China, 2007, pp. 593–604.
[24] K. L. Elmore and M. B. Richman, "Euclidean distance as a similarity metric for principal component analysis," *Monthly Weather Rev.*, vol. 129, no. 3, pp. 540–549, Mar. 2001.
[25] Y. Cai and R. Ng, "Indexing spatio-temporal trajectories with Chebyshev polynomials," in *Proc. ACM SIGMOD Int. Conf. Manage. Data (SIGMOD)*, Paris, France, 2004, pp. 599–610.
[26] C. Myers and L. Rabiner, "Connected digit recognition using a level-building DTW algorithm," *IEEE Trans. Acoust., Speech, Signal Process.*, vol. ASSP-29, no. 3, pp. 351–363, Jun. 1981.
[27] M. Vlachos, D. Gunopulos, and G. Das, "Rotation invariant distance measures for trajectories," in *Proc. ACM SIGKDD Int. Conf. Knowl. Discovery Data Mining (KDD)*, Seattle, WA, USA, 2004, pp. 707–712.
[28] L. Bergroth, H. Hakonen, and T. Raita, "A survey of longest common subsequence algorithms," in *Proc. 7th Int. Symp. String Process. Inf. Retrieval. (SPIRE)*, Madrid, Spain, 2000, pp. 39–48.
[29] M. Vlachos, G. Kollios, and D. Gunopulos, "Discovering similar multidimensional trajectories," in *Proc. 18th Int. Conf. Data Eng.*, San Jose, CA, USA, Feb. 2002, pp. 673–684.
[30] A. V. Aho, D. S. Hirschberg, and J. D. Ullman, "Bounds on the complexity of the longest common subsequence problem," in *Proc. 15th Annu. Symp. Switching Automata Theory (SWAT)*, New York, NY, USA, Oct. 1974, pp. 104–109.
[31] L. Chen and R. Ng, "On the marriage of lp-norms and edit distance," in *Proc. 13th Int. Conf. Very Large Data Bases*, Toronto, ON, Canada, vol. 30, 2004, pp. 792–803.
[32] A. Marzal and E. Vidal, "Computation of normalized edit distance and applications," *IEEE Trans. Pattern Anal. Mach. Intell.*, vol. 15, no. 9, pp. 926–932, Sep. 1993.
[33] Y. Yuan and M. Raubal, "Measuring similarity of mobile phone user trajectories—A spatio-temporal edit distance method," *Int. J. Geographical Inf. Sci.*, vol. 28, no. 3, pp. 496–520, Mar. 2014.
[34] G. Sinha and D. M. Mark, "Measuring similarity between geospatial lifelines in studies of environmental health," *J. Geographical Syst.*, vol. 7, no. 1, pp. 115–136, May 2005.
[35] D. Kondor, B. Hashemian, Y.-A. de Montjoye, and C. Ratti, "Towards matching user mobility traces in large-scale datasets," *IEEE Trans. Big Data*, vol. 6, no. 4, pp. 714–726, Dec. 2020.
[36] L. Sun, W. Zhou, B. Jiang, and J. Guan, "Multi-source trajectories similarity measure model with spatial and temporal constraints," *Syst. Eng. Electron.*, vol. 39, no. 11, pp. 2405–2413, Nov. 2017.
[37] X. Gong, Z. Huang, Y. Wang, L. Wu, and Y. Liu, "High-performance spatiotemporal trajectory matching across heterogeneous data sources," *Future Gener. Comput. Syst.*, vol. 105, pp. 148–161, Apr. 2020.
[38] F. Katsilieris, P. Braca, and S. Coraluppi, "Detection of malicious AIS position spoofing by exploiting radar information," in *Proc. 16th Int. Conf. Inf. Fusion*, Istanbul, Turkey, Jul. 2013, pp. 1196–1203.
[39] L.-Z. Sang, X.-P. Yan, Z. Mao, and F. Ma, "Restoring method of vessel track based on AIS information," in *Proc. 11th Int. Symp. Distrib. Comput. Appl. Bus., Eng. Sci.*, Guilin, China, Oct. 2012, pp. 336–340.
[40] D. J. Peters and T. R. Hammond, "Interpolation between AIS reports: Probabilistic inferences over vessel path space," *J. Navigat.*, vol. 64, no. 4, pp. 595–607, Oct. 2011.
[41] D. Zhang, J. Li, Q. Wu, X. Liu, X. Chu, and W. He, "Enhance the AIS data availability by screening and interpolation," in *Proc. 4th Int. Conf. Transp. Inf. Saf. (ICTIS)*, Banff, AB, Canada, Aug. 2017, pp. 981–986.
[42] L. Sun and W. Zhou, "A multi-source trajectory correlation algorithm based on spatial-temporal similarity," in *Proc. 20th Int. Conf. Inf. Fusion (Fusion)*, Xian, China, Jul. 2017, pp. 1–7.
[43] U. Ramer, "An iterative procedure for the polygonal approximation of plane curves," *Comput. Graph. Image Process.*, vol. 1, no. 3, pp. 244–256, Nov. 1972.
[44] D. H. Douglas and T. K. Peucker, "Algorithms for the reduction of the number of points required to represent a digitized line or its caricature," *Cartographica, Int. J. Geographic Inf. Geovisualization*, vol. 10, no. 2, pp. 112–122, Dec. 1973.
[45] Y. Huang, Y. Li, Z. Zhang, and R. W. Liu, "GPU-accelerated compression and visualization of large-scale vessel trajectories in maritime IoT industries," *IEEE Internet Things J.*, vol. 7, no. 11, pp. 10794–10812, Nov. 2020.
[46] J. Liu, H. Li, Z. Yang, K. Wu, Y. Liu, and R. W. Liu, "Adaptive douglas-peucker algorithm with automatic thresholding for AIS-based vessel trajectory compression," *IEEE Access*, vol. 7, pp. 150677–150692, 2019.
[47] Y. C. Hou, P. Wang, X. Liu, and J. Teng, "Algorithm study for stay points recognition of spatial trajectory based on velocity," *Geography Geo-Inf. Sci.*, vol. 32, no. 6, pp. 63–68, Jun. 2016.

CHAO LIU received the B.S. degree in geographic information science (GIS) from Shandong Normal University, Jinan, China, in 2018. He is currently pursuing the M.S. degree in cartography and GIS with the College of Geomatics, Shandong University of Science and Technology. His current research interests include ship data mining and ocean data distributed storage.

JINLEI WANG was born in Shandong, China, in 1982. He received the B.S. degree from the Qingdao University of Technology and the M.S. degree from the Ocean University of China. He is currently an Intermediate Engineer with North China Sea Data and Information Service, Ministry of Natural Resources. His research interests include construction, and application of information system for marine management.

AICHAO LIU received the M.S. degree from the Shandong University of Science and Technology. He is currently a Senior Engineer, the Deputy Director of the Information and Archives Department, North China Sea Marine Forecasting Center, Ministry of Natural Resources, and the Director of the Shandong Intelligent Ocean Engineering Association. His research interests include marine environment information research and construction.

YONGNING CAI was born in Weifang, China, in 1987. He received the M.S. degree from the Shandong University of Science and Technology, Shandong, in 2013. He is currently an Intermediate Engineer with the Jinan Research Institute of Surveying and Mapping. His research interests include GIS big data application analysis, and geographic information application and development.

BO AI was born in Hubei, China, in 1979. He received the B.S. and M.S. degrees from Wuhan University, Wuhan, in 2005, and the Ph.D. degree in GIS from the Shandong University of Science and Technology, in 2011. He is currently an Associate Professor. He is also the Director of the Geographic Information Department, Shandong University of Science and Technology. His research interests include ocean spatial-temporal modeling, maritime search, and rescue decision analysis. He has hosted the National Science Foundation of China (NSFC) and the Ph.D. Programs Foundation of Ministry of Education of China. As a Key Personnel, he participated in NSFC, the National High-Tech Research and Development Program of China (863 Program) five times. He has published more than 30 articles, including 15 articles indexed by SCI/EI. His technological achievement long-term prediction of Chinese offshore dynamic environment and system development received the Second Prize of the 2016 Geographic Information Technology Progress Award.